JOURNAL OF AGRICULTURAL AND FOOD CHEMISTRY
ARTICLE

J. Agric. Food Chem. 2010, 58, 235–241 235
DOI:10.1021/jf9031684

Combination Treatment with Luteolin and Quercetin Enhances Antiproliferative Effects in Nicotine-Treated MDA-MB-231 Cells by Down-regulating Nicotinic Acetylcholine Receptors

Yung-Leun Shih,[†,‡] Hui-Ching Liu,[‡] Ching-Shyang Chen,[§] Chung-Huei Hsu,[#] Min-Hsiung Pan,[⊥] Hui-Wen Chang,[⊗] Chien-Hsi Chang,[⊗] Feng-Chia Chen,[▽] Chi-Tang Ho,[○] Yi-Yuan Yang,*[,‡,▽,∥] and Yuan-Soon Ho*[,‡,⊗,∥]

[†]Department of Pathology and Laboratory Medicine, Shin Kong Wu Ho-Su Memorial Hospital, Taipei, Taiwan, [‡]Graduate Institute of Medical Sciences, College of Medicine, Taipei Medical University, Taipei, Taiwan, [§]Department of Surgery, School of Medicine, Taipei Medical University Hospital, Taipei, Taiwan, [#]Department of Nuclear Medicine, School of Medicine, Taipei Medical University Hospital, Taipei, Taiwan, [⊥]Department of Seafood Science, National Kaohsiung Marine University, Kaohsiung, Taiwan, [⊗]Department of Laboratory Medicine, Taipei Medical University Hospital, Taipei, Taiwan, [▽]Department of Laboratory Medicine, Taipei Municipal Wan Fang Hospital, Taipei, Taiwan, and [○]Department of Food Science, Rutgers University, New Brunswick, New Jersey 08901. [∥] The second and ninth authors contributed equally to this work.

Large-scale epidemiological cohort studies performed in the United States indicate that breast cancer risk is associated with active and passive smoking. As of yet, however, there is no direct evidence of antitumor effects by agents that block the effect of tobacco compound nicotine (Nic) on relevant nicotinic receptors (nAChR) involved in breast tumorigenesis. In the present study, the expression profiles of different nAChR subunits in the human breast cancer cell line (MDA-MB-231) were characterized by RT-PCR. Nic (>0.1 μM, 6 h) significantly increased α9-nAChR mRNA and protein expression levels in human breast cancer cells (MDA-MB-231 cells). On the other hand, combined treatment with luteolin (Lut, 0.5 μM) and quercetin (Que, 0.5 μM) profoundly decreased MDA-MB-231 proliferation by down-regulating α9-nAChR expression. MDA-MB-231 cells were cultured in soft agar to evaluate anchorage-independent colony formation; combined treatment of Lut + Que inhibited Nic-induced MDA-MB-231 colony formation. Interestingly, the number of colonies formed was profoundly reduced in α9-nAChR knockdown (Si α9) cells in the combined (Lut + Que)-treated group as compared to the relevant control groups. Such results show that Lut- or Que-induced antitransforming activities were not limited to specific inhibition of the α9-nAChR receptor. Both α5- and α9-nAChR appear to be important molecular targets for Lut- and Que-induced antitumor effects in human breast cancer cells.

KEYWORDS: Luteolin; quercetin; breast cancer; nicotinic receptor

INTRODUCTION

Breast cancer is the second leading cause of cancer death among women in the United States. Cigarette smoking may contribute to a woman's risk of developing breast cancer (*1*). Large-scale epidemiological cohort studies indicate that breast cancer risk is associated with cigarette smoking (*2*, *3*). Cigarette smoke is a complex mixture of over 4000 chemical constituents. However, studies focus on the carcinogenic roles of nicotine (Nic) and its metabolic active carcinogenic compounds, including 4-(methylnitrosamino)-1-(3-pyridyl)-1-butanone (NNK). Previous studies demonstrated that >80% of inhaled Nic is absorbed after smoking (*4*). The carcinogenic effects of smoking carcinogens such as NNK have been examined by previous studies using soft agar transformation assays and a xenografted nude mouse animal model that demonstrate transformation of noncancerous human breast epithelial (MCF-10A) cells to transformed cancerous cells (*5*, *6*). Repeated exposure of normal MCF-10A cells to smoking carcinogens sensitized cells to growth factor-promoted cell proliferation and increased their anchorage-independent colony formation (*6*).

The fact that cigarette smoking is a major risk factor in some human cancers suggests that smoking carcinogens such as Nic and NNK may act in a specific receptor-dependent manner to induce carcinogenic transformation of cells (*7*−*10*). The physiological ligand of Nic receptor (nAChR) is acetylcholine; tobacco carcinogens such as Nic and NNK are agonists of

*Corresponding authors [(Y.-S.H.) Graduate Institute of Biomedical Technology, Taipei Medical University, No. 250 Wu-Hsing St., Taipei 110, Taiwan (telephone +886-2-2736-1661, ext. 3327; fax +886-2-2739-3422; e-mail hoyuansn@tmu.edu.tw); (Y.-Y.Y.) Graduate Institute of Biomedical Technology, Taipei Medical University, No. 250 Wu-Hsing St., Taipei 110, Taiwan (telephone +886-2-2736-1661, ext 3325; fax +886-2-2739-3422; e-mail yangyuan@tmu.edu.tw)].

Published on Web 11/18/2009

nAChRs (*11*, *12*). Therefore, inhibition of nAChR-mediated signals represents a potential effective strategy for improving cancer chemotherapy, as well as a potential chemopreventive agent.

Epidemiological evidence suggests a protective effect of polyphenols from fruits and vegetables on the occurrence of human cancers (*13*). Another study demonstrated that tea and tea polyphenols may be preventive against various cancers, including breast cancer (*14*, *15*). Flavonoids are polyphenolic compounds that represent integral components of the human diet. They are universally present as constituents of flowering plants, particularly those that are used for food. Flavonoids are phenyl-substituted chromones (benzopyran derivatives) consisting of a 15-carbon basic skeleton (C6−C3−C6) and a chroman (C6−C3) nucleus (represented by the benzo ring and the heterocyclic ring) that is also shared by the tocopherols; a phenyl (aromatic ring) substitution usually exists at the 2-position. Experimental animal studies indicate that certain dietary flavonoids possess antitumor activity (*16*). The hydroxylation pattern of the aromatic ring of the flavones and flavonols, including that of luteolin (Lut) and quercetin (Que), critically influences their activities, especially with respect to inhibition of protein kinase activity and cell proliferation (*17*). The dietary flavonols (Que) and flavones (Lut) target cell surface signal transduction enzymes, such as protein tyrosine and focal adhesion kinases and also affect angiogenesis, making them promising candidates as anticancer agents (*18*).

Thus, nAChR in human breast cancer cells may be adapted as a potential molecular target for clinical therapeutic purposes (*19*). In addition, acquisition of drug resistance is a considerable challenge in breast cancer therapy. Nic protects cells against apoptosis. Therefore, we suggest that Que and Lut could act as nAChR antagonists that could be used in combination with established chemotherapeutic drugs to enhance therapeutic responses to chemotherapy (*19*, *20*).

In this study, we demonstrate for the first time that Que and Lut inhibit human breast cancer cell proliferation through inhibition of cell surface Nic receptors and that inhibition of α9-nAChR subunit expression in human breast cancer cells by Lut and Que significantly inhibits anchorage-independent colony formation. To explore the potential anticarcinogenic effects of Lut and Que on α9-nAChR subunit expression in human breast cancer cells, we established α9-nAChR siRNA knockdown MDA-MB-231 cancer cells. Lut- or Que-induced antitransforming activities were not limited to specific inhibition of the α9-nAChR receptor. Both the α5- and α9-nAChR may be important molecular targets for Lut- or Que-induced antitumor effects on human breast cancer (MDA-MB-231) cells. Despite the considerable research performed in this study, the intracellular molecules directly linked to tobacco carcinogen-induced breast epithelial cell transformation remain unknown.

MATERIALS AND METHODS

Cell Culture. Human mammary gland epithelial adenocarcinomas (MCF-7, MDA-MB-231, and BT-483) and human normal mammary gland epithelial fibrocystic cell lines (MCF-10A) were obtained from the American Tissue Cell Culture collection (ATCC no. HTB22, HTB26, HTB124, and HTB131). MCF-10A cells were maintained in complete MCF-10A culture medium [1:1 mixture of Dulbecco's modified Eagle's medium (DMEM) and Ham's F12 supplemented with 100 ng/mL cholera enterotoxin, 10 μg/mL insulin, 0.5 μg/mL hydrocortisol, and 20 ng/mL epidermal growth factor] (Life Technologies, Rockville, MD). MCF-7 and MDA-MB-231 cells were maintained in DMEM, whereas BT-483 cells were maintained in RPMI-1640. Cell growth, proliferation, and viability were determined by the 3-(4,5-dimethylthiazol-2-yl)-2,5-diphenyltetrazolium (MTT) assay. An aqueous stock solution of 10 mM Nic and NNK (Chemsyn, Lenexa, KS) was prepared in dimethyl sulfoxide (DMSO).

RNA Isolation and RT-PCR Analysis. Total RNA was isolated from human cell lines using Trizol (Invitrogen, Carlsbad, CA), according to the manufacturer's protocol. nAChR subunit-specific primers were synthesized by MB Mission BioTech (Taipei, Taiwan) as described in a previous paper (*9*) (Supporting Information Table 1). PCR amplicons were analyzed on a 1.2% agarose gel (Amresco, Inc., Solon, OH) stained with ethidium bromide. α9-nAChR mRNA intensity was measured and normalized to β-glucuronidase (GUS) expression (*21*). Pictures of the bands were taken using an Infinity-α digital imaging system (Vilber Lourmat, France), and band intensities were determined using PhotoCapt version 11.01.

Protein Extraction, Western Blotting, and Antibodies. To prepare protein samples, the cells were washed once with ice-cold phosphate-buffered saline and lysed on ice in cell lysis buffer (50 mM Tris-HCl, pH 8.0, 120 mM $NaCl_2$, 0.5% Nonidet P-40, 100 mM sodium fluoride, and 200 μM sodium orthovanadate) containing protease inhibitors as previously described (*22*). Protein (50 μg) from each sample was resolved by 12% SDS−polyacrylamide gel electrophoresis, transferred, and analyzed by Western blotting. Antibodies were purchased from the following vendors: antitotal AKT, anti-ERK, antiphospho ERK, and protein A/G agarose beads were from Santa Cruz Biotechnology (Santa Cruz, CA); anti-GAPDH and anti-α9-nAChR antibodies were from ABcam (Cambridge, U.K.); and antiphospho AKT (Ser^{473}) antibody was from Cell Signaling Technology (Danvers, MA). The secondary antibodies, alkaline phosphatase-coupled anti-mouse and anti-rabbit IgG, were purchased from Santa Cruz Biotechnology. Specific protein complexes were identified by incubation with the colorigenic substrates nitro blue tetrazolium (NBT) and 5-bromo-4-chloro-3-indolylphosphate (BCIP) (KPL, Inc., Gaithersburg, MD). In each experiment, proteins were also probed with an anti-GAPDH antibody as a protein loading control.

Soft Agar Cloning Assay. The base layer consisted of 0.9% low-gelling-point SeaPlaque agarose (Sigma, St. Louis, MO) in culture medium. Soft agar consisting of 0.4% SeaPlaque agarose in culture medium was mixed with 1×10^4 MDA-MB-231 cells and plated on top of the base layer in 60 mm culture dishes. Soft agar cultures were maintained at 37 °C, and colonies that appeared were counted using a Leica DMI 4000B Microscope Imaging System (Leica Microsystems, Wetzlar, Germany).

RNA Interference. α9-nAChR expression was ablated in breast cancer cells with at least two independent small interfering RNAs (siRNAs). The target sequences of α9-nAChR mRNA were selected to suppress α9-nAChR gene expression. Scrambled sequences of each siRNA were used as controls (Supporting Information Table 1). After BLAST analysis to verify that there were no significant sequence homologies with other human genes, the selected sequences were inserted into *Bgl*II/*Hin*dIII-cut pSUPER vectors to generate the pSUPER-Si α9-nAChR and pSUPER-scramble vectors. All constructs were confirmed by DNA sequence analysis. The transfection protocol has been described previously (*23*). Briefly, 1.5×10^5 cells were washed twice with phosphate-buffered saline and mixed with 0.5 μg of plasmid. One pulse was applied for 20 ms under a fixed voltage of 1.6 kV on a pipet-type microporator MP-100 (Digital Bio, Seoul, Korea).

Generation of Stable nAChR-Knockdown Cell Lines. At least three clones of the MDA-MB-231 cell lines stably expressing the siRNA were generated. All experiments were performed using multiple subclones of each cell line, with consistent results. The pSUPER-Si α9-nAChR and pSUPER-scramble vectors were transfected, and stable integrants were selected 72 h later with G418 (4 mg/mL). After 30 days in selective medium, two G418-resistant clones, referred to as pSUPER-Si α9-nAChR, were isolated. These clones demonstrated >80% reduction in mRNA and protein levels as compared to control clones (pSUPER-scramble).

Plasmid Constructions. All nAChR α9 promoter−luciferase gene fusions were made in the pGL3-Basic vector (Promega), introducing the suitable α9 promoter fragments in its polylinker upstream of the luciferase gene. These fragments were generated with restriction enzymes and cloned directly into pGL3-Basic or subcloned first in pBluescript and then transferred to pGL3-Basic. Deletion analysis of the most

promoter-proximal region was performed by generating either appropriate restriction enzyme fragments or PCR fragments with suitable sense oligonucleotides and an antisense primer (5′-tatagaggctcaggaaaaag-3′) that anneals to the pGL3-Basic vector downstream of the transcription start site.

Luciferase Activity Assay. MDA-MB-231 cells were plated in 6-well plates. Cells were transiently cotransfected the next day with 1.5 μg of α9-nAChR full-length promoter in the pGL3-Basic plasmid and 0.1 μg of RLTK plasmid (Promega, Madison, WI) using a microporator MP-100 (Digital Bio), according to the manufacturer's instructions. After incubation for 24 h, the medium was changed to culture medium containing 10% FBS or 0.1% FBS with or without Nic. Cells were lysed 24 h later with 1× Reporter Lysis Buffer (Promega) and stored frozen at −20 °C overnight. Luciferase activity was determined by testing 50 μL of cell lysate and 50 μL of Luciferase Assay Reagent (Promega) using a HIDEX Chameleon microplate reader. Relative luciferase units were normalized to renilla luciferase from the same cell lysates. Each luciferase assay experiment was performed three times.

Chromatin Immunoprecipitation (ChIP) Assay. ChIP assays of cultured cells were performed as described previously. Briefly, after various regimens of nicotine treatment, the cells were fixed by adding a final concentration of 1% directly to the cell culture medium at 25 °C for 15 min. The cross-linking reaction was terminated by adding glycine (final concentration = 0.125 M) for 5 min, and the cells were collected into a new Eppendorf tube. The cell lysate was sonicated three times with 10 s bursts to yield input DNA enriched for fragments around 1000 bp in size. The nuclear factor kappa B (NFκB) antibody (Santa Cruz Biotechnology Inc.) was used for the immunoprecipitation reactions. Specific primers (Supporting Information Table 1) for the α9-nAChR promoter region amplified a region from −960 to −1 for 32 cycles. The PCR products were then separated and analyzed by agarose gel electrophoresis.

Statistics. All data were expressed as the mean value ± SEM. Comparisons were subjected to one-way analysis of variance (ANOVA) followed by Fisher's least significant difference test. Significance was accepted at $P < 0.05$.

RESULTS

nAChR Expression in a Human Breast Cancer Cell Line. Recent studies have demonstrated that Nic binds to nAChR subunits and that this interaction may mediate the carcinogenic effects of this tobacco component (*9*, *22*). To test whether Nic induced breast cancer cell proliferation through its relevant receptor (α9-nAChR), MDA-MB-231 cells were treated with Nic, and the levels of α9-nAChR mRNA were measured (**Figure 1A**). RT-PCR analysis indicated that a significant increase in α9-nAChR mRNA level occurred in MDA-MB-231 cells 6 h after Nic treatment (**Figure 1A**, upper panel, lane 2). Interestingly, the α9-nAChR mRNA level returned to the basal level 24 h after exposure to Nic (**Figure 1A**, upper panel, lane 4). Accordingly, the 6 h time point was selected to test the dose dependency of Nic-induced α9-nAChR mRNA expression in MDA-MB-231 cells. The results show that a relative 1.62-fold α9-nAChR mRNA level was induced by Nic (>0.1 μM) in MDA-MB-231 cells. Similar results were also seen at the protein level; the amount of immunoreactive α9-nAChR in MDA-MB-231 cells that were treated with Nic increased in a dose-dependent manner (**Figure 1B**, left, lane 2).

Effects of Lut and Que on Inhibition of Nic-Induced Breast Cancer Cell Proliferation. To test whether Nic plays a role in cancer cell proliferation through its relevant receptor (α9-nAChR), human breast cancer cells (MDA-MB-231) that express α9-nAChR were treated with Nic (1 μM) in the presence or absence of either Lut or Que, and growth proliferation assays were performed on the cells (**Figure 2A**). Our results show that the higher concentration of Lut and Que (1 μM for 24 h) significantly down-regulated α9-nAChR mRNA expression [**Figure 2A**, bar 2 vs 4 and 6 (∗, $P < 0.05$)]. We also found that Lut and Que

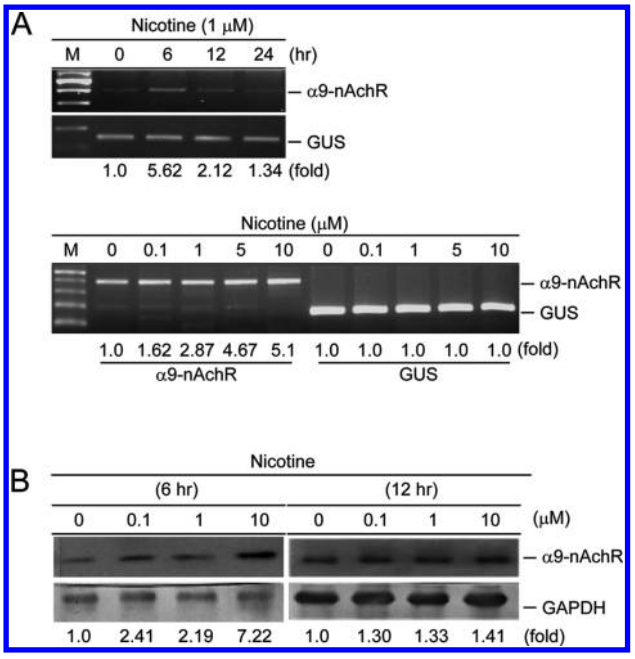

Figure 1. Nic-induced nicotinic receptor up-regulation in human breast cancer cells. (**A**) Nic-induced α9-nAChR mRNA expression in MDA-MB-231 cells. MDA-MB-231 cells were treated with Nic (1 μM) for various intervals of time (upper panel). For dose-dependent experiment, MDA-MB-231 cells were treated with Nic (0.1−10 μM) for 6 h (lower panel). Total RNA was isolated from the cells, and RT-PCR analysis was performed for α9-nAChR mRNA analysis. (**B**) Nic-induced α9-nAChR protein expression in MDA-MB-231 cells. MDA-MB-231 cells were treated with Nic for various intervals of time. The protein expression level of α9-nAChR was detected by immunoblotting analysis.

significantly inhibited Nic-induced cell proliferation in a time-dependent manner [**Figure 2B**, upper panel (∗,$P < 0.05$)].

Interestingly, we found that combined treatment with both agents at half the concentration (0.5 μM) synergistically down-regulated α9-nAChR mRNA expression [**Figure 2A**, bar 8 vs 4 and 6, respectively (#, $P < 0.05$)]; a corresponding decrease in cell proliferation was also observed (**Figure 2B**). To test whether the cytotoxic effect was cancer cell-specific, normal human breast epithelial (MCF-10A) cells were treated in the same manner, and cell proliferation assays were performed (**Figure 2B**). Our results show that the antiproliferative effects induced by the combined treatment of Lut and Que occurred preferentially in human breast cancer (MDA-MB-231, MCF-10A, and BT-483) cells. All of these results indicate that the cytotoxic effect Lut and Que in human breast cancer cells correlated with α9-nAChR inhibition.

Effects of Lut and Que on the Inhibition of Nic-Induced Breast Cancer Cell Colony Formation in Soft Agar. We further tested the effects of Lut and Que on the inhibition of Nic-induced breast cancer cell colony formation. Nic-treated MDA-MB-231 cells were cultured in soft agar for 21 days (**Figure 3A**) (*5*, *24*). Soft agar assays were conducted, and the number of transformed colonies was determined in MDA-MB-231, α9-nAChR knockdown (Si α9), and scrambled vector control (Sc) cells (**Figure 3B**). After treatment with Nic, more transformed colonies were observed in wild-type MDA-MB-231 and scrambled vector control (Sc) cells compared with the α9-nAChR knockdown (Si α9) MDA-MB-231 cells [**Figure 3A**, bar 1 vs 2 (∗, $P < 0.05$)]. To test whether Nic-induced colony formation occurred through activation of its cognate receptor (α9-nAChR), human breast cancer cells (MDA-MB-231) that expressed α9-nAChR, α9-nAChR knockdown (Si α9), and scrambled vector control (Sc)

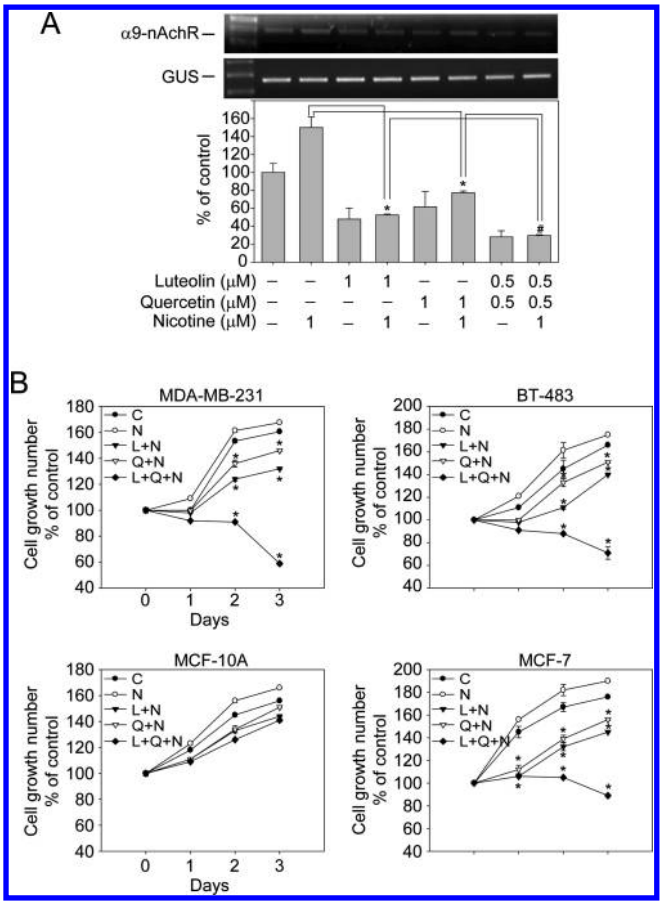

Figure 2. Effects of Lut and Que on the inhibition of Nic-induced breast cancer cell proliferation. (**A**) MDA-MB-231 cells were treated with Nic (1 μM) in the presence or absence of Lut (1 μM) and Que (1 μM) for 24 h. After treatment, total RNA was isolated and RT-PCR analysis was performed for the determination of α9-nAChR mRNA level. In the combination-treated group, half the concentration of Lut (0.5 μM) and Que (0.5 μM) was added to MDA-MB-231 cells, and the α9-nAChR mRNA level was subsequently detected by RT-PCR analysis. (**B**) Human cancerous (MDA-MB-231, MCF-7, and BT483) and normal (MCF-10A) breast cell lines were treated with either Nic (1 μM) or vehicle alone with or without Lut (1 μM) and Que (1 μM) for 24 h. In the combination-treated group, half the concentration of Lut (0.5 μM) and Que (0.5 μM) was added to both cells, and cell growth was measured by the MTT assay with an OD (540 nm) at the indicated time points.

cells were treated with Nic in the presence or absence of Lut (1 μM) or Que (1 μM), and soft agar colony formation assays were performed (**Figure 3B**). Both Lut (1 μM) and Que (1 μM) significantly inhibited the formation of transformed colonies when compared to Nic-treated cells that did not receive flavonoid treatment [**Figure 3B**, bar 2 vs 4 and 6 (∗, $P < 0.05$)]. We further demonstrated that combined treatment with lower concentrations of both agents (0.5 μM) synergistically inhibited colony formation [**Figure 3B**, bar 8 vs 4 and 6 (#, $P < 0.05$)]. Interestingly, we also found that colony formation was profoundly inhibited in α9-nAChR knockdown cells (**Figure 3B**, middle panel) compared to control cells (**Figure 3B**, upper and lower panels).

Nic-Induced Cancer Cell Proliferation Occurs through Activation of AKT and ERK Signaling Pathways in MDA-MB-231 Cells. To determine whether the activation of upstream stimulatory factors such as AKT (*25*) plays a role in Nic-induced cell proliferation, MDA-MB-231 cells were treated with Nic (1 μM) for various times, and Western blot analysis was performed. The results show

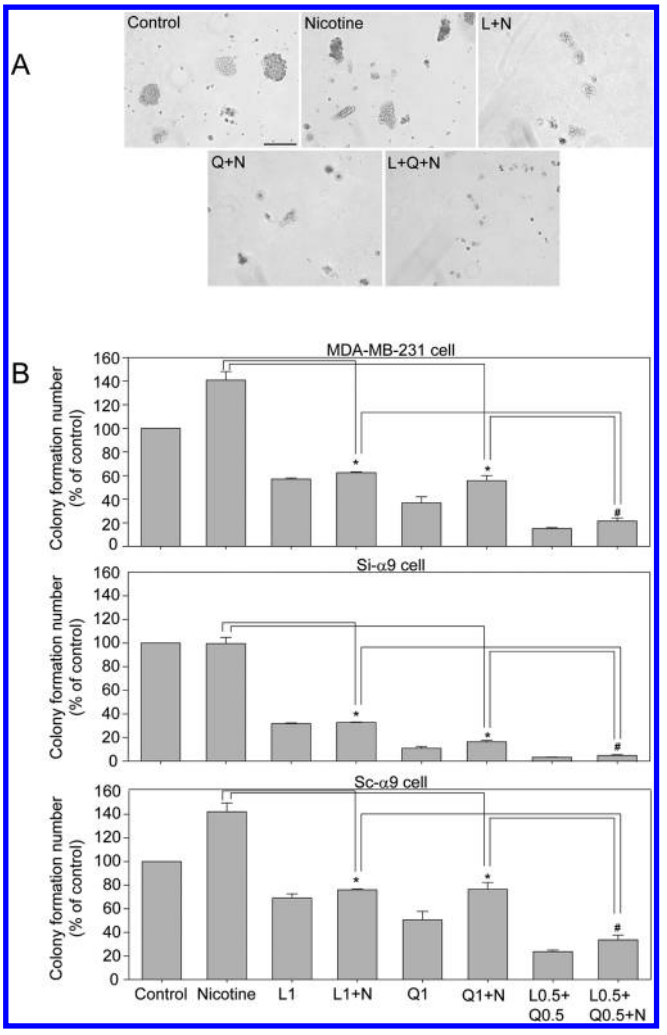

Figure 3. Effects of Lut and Que on the inhibition of Nic-induced breast cancer cell colony formation in soft agar. (**A**) Anchorage-independent growth of Lut- and Que-treated MDA-MB-231 cells in soft agar. The MDA-MB-231 cells were treated with Nic (1 μM) or vehicle alone with or without Lut (1 μM) and Que (1 μM) using methods described previously (*5*). In the combination-treated group, half the concentration of Lut (0.5 μM) and Que (0.5 μM) was added to MDA-MB-231 cells. The gross morphology of MDA-MB-231 cell colonies on culture plates is shown. These colonies exhibit subtle changes in their morphology, which include a slight disaggregation compared to the untreated MDA-MB-231 cells. Bar = 200 μm. (**B**) The number of colonies scored from the soft agar plates. The wild-type MDA-MB-231, α9-nAChR Si RNA knockdown (Si-α9), and scrambled sequence control (Sc-α9) cells were seeded in soft agar and treated with Nic in the presence or absence of Lut and Que. The colonies were counted in a 1 × 3 cm area on each plate. Data are the mean ± SE of three independent experiments. Significance was accepted at $P < 0.05$. ∗, the combination Lut+Nic- and Que+Nic-treated groups were significantly different from the Nic-treated group. #, the combined Lut+Que+Nic-treated groups were significantly different from the Lut+Nic- and Que+Nic-treated groups.

that Nic treatment significantly increased the levels of p-AKT (Ser^{473}) and p-ERK in MDA-MB-231 cells within 6 h and maintained this up-regulation for the duration of the experiment (24 h) (**Figure 4A**). Time-dependent increases in α9-nAChR and cyclin D1 protein levels were also detected in MDA-MB-231 cells (**Figure 4A**). These results are of clinical importance because a previous study demonstrated that the steady state serum concentration of Nic in smokers was 200 nM and acutely reached the

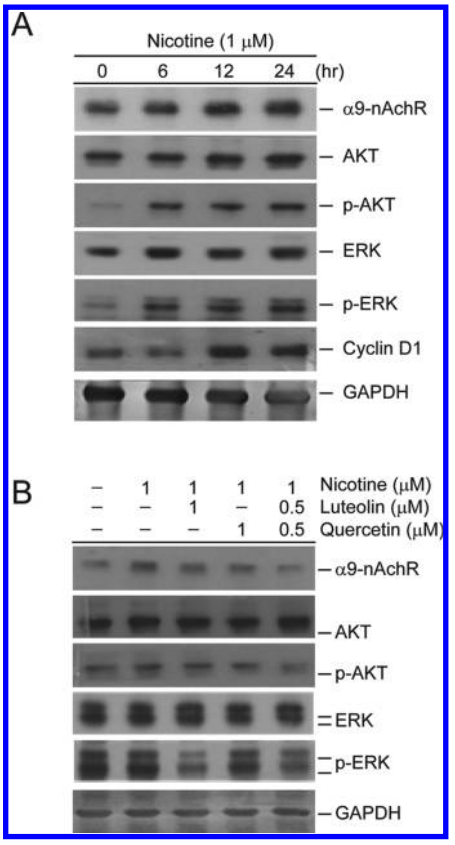

Figure 4. Effect of Lut and Que on Nic-induced cell survival signal proteins. (**A**) MDA-MB-231 cells were treated with Nic (1 μM) for 6−24 h. Protein extracts (100 μg/lane) were separated by SDS-PAGE, probed with specific antibodies, and detected using the nitro blue tetrazolium and 5-bromo-4-chloro-3-indolyl-phosphate systems. Membranes were also probed with an anti-GAPDH antibody to correct for differences in protein loading. (**B**) The MDA-MB-231 cells were treated with Nic (1 μM) or vehicle alone with or without Lut (1 μM) and Que (1 μM), and the samples were processed using the immunoblotting methods described above. In the combination-treated group, half the concentration of Lut (0.5 μM) and Que (0.5 μM) was added to MDA-MB-231 cells.

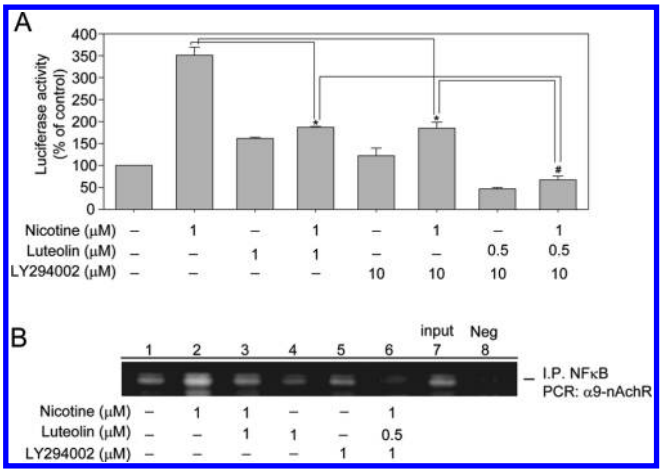

Figure 5. Effect of Lut and Que on the Nic-induced α9-nAChR promoter activity in MDA-MB-231 cells. (**A**) MDA-MB-231 cells were transfected with a construct containing the full-length fragment of the α9-nAChR promoter for 6 h in combination with Nic (1 μM) treatment. Cells were also pretreated with 10 μM LY294002 for 60 min and subsequently exposed to Nic (1 μM) with or without Lut (0.5 μM) for an additional 6 h. The luciferase reporter was measured and normalized to renilla luciferase activity as a transfection efficiency control. (**B**) MDA-MB-231 cells were treated with Nic (1 μM) or vehicle alone with or without Lut (1 μM) for 24 h. To test whether PI3K was involved in the α9-nAChR promoter activation, cells were pretreated with LY294002 (10 μM, PI3K inhibitor) for 60 min and subsequently treated with Nic and Lut for an additional 24 h. Anti-NFκB was used to perform the ChIP assay. DNA extracts were analyzed with primers for the α9-nAChR promoter PCR. Total cell input is labeled as "input", and a nonspecific IgG antibody was used as a negative control and is labeled "Neg".

range of 10−100 μM in serum and 1 mM in saliva immediately after smoking (*9*).

We next examined the combined inhibitory effects of Lut and Que on AKT and ERK activation in MDA-MB-231 cells. MDA-MB-231 cells were treated for 24 h with Nic (1 μM) in the presence of either Lut (1 μM) or Que (1 μM) or a combination (0.5 μM each) of both agents (**Figure 4B**). The levels of p-AKT (Ser^{473}) and p-ERK were detected by Western blotting. The results demonstrate that combined treatment with Lut and Que synergistically inhibited Nic-induced AKT (Ser^{473} phosphorylation) (**Figure 4B**, lane 2 vs 5). Interestingly, Nic-induced ERK phosphorylation was inhibited in Lut-treated but not in Que-treated cells (**Figure 4B**, lane 3 vs 4). These results indicate that an upstream kinase (such as PI3K), acting through AKT, plays a significant role in Nic-induced cell proliferation.

Lut Inhibits Nic-Induced AKT Phosphorylation through Activation of MAPK Kinase in MDA-MB-231 Cells. A recent study demonstrated that pretreatment of cells with the PI3-kinase (PI3K)/AKT inhibitor LY294002 markedly inhibited Nic-stimulated non-small-cell lung carcinoma cell proliferation through α7-nAChR-mediated signals (*26*). As described above, our study shows that Nic-induced up-regulation of α9-nAChR was inhibited by Lut and Que through inactivation of pAKT but not pERK (**Figure 4B**, lanes 3−5). To study the transcriptional regulation of α9-nAChR in response to Nic and its antagonist compounds (such as Lut), a 1.1 kb genomic fragment encompassing the human α9-nAChR promoter was inserted upstream of the luciferase reporter gene. Luciferase activity obtained with the vector alone without the α9-nAChR promoter was defined as 1-fold (basal level). Experiments utilizing the full-length construct show that α9-nAChR promoter activity was significantly induced (> 3-fold) in MDA-MB-231 cells by Nic (1 μM) treatment for 6 h [**Figure 5A**, bar 1 vs 2 (∗, $P < 0.05$)]. MDA-MB-231 cells were also pretreated with the PI3K inhibitor (Ly294002, 10 μM) for 60 min in the presence or absence of either Lut (1 μM) or Nic (1 μM) for an additional 6 h. Pretreatment with Ly294002 abrogated most of the Nic-induced α9-nAChR promoter luciferase activity [**Figure 5A**, bar 2 vs 6 (∗, $P < 0.05$)]. Similar results were also seen in Nic+Lut-treated cells [**Figure 5A**, bar 2 vs 4 (∗, $P < 0.05$)].

To test whether Lut-mediated inhibition of the PI3K/AKT pathway was critical for transcriptional regulation of α9-nAChR in response to Nic treatment, MDA-MB-231 cells were pretreated with Ly294002 and then treated with Lut (0.5 μM) plus Nic (1 μM) for an additional 6 h. The results showed that combined treatment with both Ly294002 and Lut synergistically inhibited the Nic-induced α9-nAChR promoter-driven luciferase activity [**Figure 5A**, bar 4 vs 8 (#, $P < 0.05$)]. These results suggest that the PI3K/AKT pathway may control α9-nAChR transcriptional regulation.

Nic-Induced Transcriptional Activation of α9-nAChR Gene Expression by NFκB. Our previous study demonstrated that NFκB plays an important role in the up-regulation of cyclin D1, a cellular regulatory protein that confers increased proliferative capacity to Nic-stimulated normal human bronchial epithelial cells and small airway epithelial cells (*22*). To determine whether NFκB is a transcription factor that directly binds to the

α9-nAChR promoter in response to Nic treatment, ChIP assays were performed in MDA-MB-231 cells. Results demonstrate that binding of NFκB to the α9-nAChR promoter is increased 6 h after Nic (1 μM) treatment in MDA-MB-231 cells (**Figure 5B**, lane 2). Combined treatment with Lut or Ly294002 attenuated Nic-induced NFκB binding to the α9-nAChR promoter (**Figure 5B**, lane 2 vs 6).

DISCUSSION

Cigarette smoking is the chief risk factor in many types of human cancers, suggesting that smoking carcinogens such as Nic and NNK may act in a specific receptor-dependent manner (*7*−*10*). Our previous study demonstrated that Nic induces normal human bronchial epithelial and small airway epithelial cell proliferation by activating α3/α4 nAChR subunits (*22*). The nAchRs have recently emerged as candidate pathogenic factors in tobacco-related morbidity because they exert regulatory roles in various biological processes including cell growth, motility, and differentiation (*27*−*29*). A recent study from our group further demonstrated that inhibition of α7-nAChR attenuated NNK-induced colon cancer cell migration (*30*). On the basis of these results, we hypothesized that inhibiting nAChR-mediated signals may represent an effective strategy for improving cancer chemotherapeutic or chemopreventive therapies. In this study, Lut and Que each inhibited the Nic-induced α9-nAChR mRNA expression level in MDA-MB-231 cells. A combined treatment with lower concentrations of both agents (0.5 μM) synergistically enhanced inhibition of cancer cell growth and soft agar transformation activity. Notably, we further demonstrated that colony formation in soft agar (anchorage-independent) experiments is profoundly inhibited by Lut and Que in α9-nAChR knockdown cells. These results suggest that the observed Lut- or Que-induced antitransforming activities are not α9-nAChR receptor-specific. Another nicotinic receptor (α5-nAChR) that has been detected in MDA-MB-231 cells may be involved.

Although Nic-induced signaling pathways have been reported in various types of human cancer cells, the molecular mechanism underlying the effects of Nic in breast cancer cells remains unclear. In the present study, Nic-induced AKT and ERK protein activation was detected in MDA-MB-231 cells. Combined treatment with Lut and Que synergistically inhibited the AKT activation. However, Nic-induced ERK activation was blocked solely by Lut. Such results demonstrate that AKT survival signals play an important role in the Nic-mediated carcinogenic process in human breast cancer cells. Results from CHIP assays also showed that Lut blocks the NFκB-mediated transcriptional activation of the a9-nAChR promoter. Inhibiting AKT by LY294002 (PI3K inhibitor) attenuated the NFκB/a9-nAChR promoter binding activity. This result suggests that PI3K kinase is involved in IκBα phosphorylation, which then promotes the nuclear translocation of NFκB (*22*).

Flavonoids may protect against cancer development through several biological mechanisms (*13*). However, epidemiologic studies on dietary flavonoids and cancer risk have yielded disparate results (*31*). Recently, the natural flavone diosmetin was shown to inhibit proliferation of the breast adenocarcinoma cell line MDA-MB 468 and the normal breast cell line MCF-10A cells; diosmetin was found to be selective for the cancer cells with slight toxicity against the normal breast cells. Diosmetin was metabolized to the structurally similar flavone Lut in MDA-MB 468 cells, whereas no metabolism was seen in MCF-10A cells (*32*). These authors also showed that diosmetin is metabolized to the more active molecule Lut by the CYP1 family of enzymes in estrogen receptor-positive MCF-7 cells (*33*). Such results could explain our observation that combined treatment with Lut and Que inhibited MDA-MB-231 cell proliferation more profoundly than normal breast epithelial cell (MCF-10A) proliferation. Lut exhibits a wide spectrum of antitumor activities. Another study demonstrated that Lut can sensitize human breast cancer cells to doxorubicin (*34*). In contrast, Que inhibits tumor invasion by suppressing PKC δ/ERK/AP-1-dependent matrix metalloproteinase-9 activation in breast carcinoma cells (*35*). In a previous study, we evaluated the antitumor potential of Lut (30 mg/kg, po) and cyclophosphamide (Lut+CYC) when orally administered for 20 days as well as CYC when administered for 10 days against induced mammary carcinogenesis in Wistar rats. Combination treatment of Lut+CYC (10 mg/kg, ip) significantly reduced the incidence rate of breast tumors induced by 7,12-dimethylbenz(*a*)anthracene and decreased tumor volume without changing the total body weight of the experimental animals (*36*).

ABBREVIATIONS USED

ChIP, chromatin immunoprecipitation; DMSO, dimethyl sulfoxide; GUS, β-glucuronidase; Lut, luteolin; MTT, 3-(4,5-dimethylthiazol-2-yl)-2,5-diphenyltetrazolium; nAChR, nicotinic receptor; NFκB, nuclear factor kappa B; Nic, nicotine; NNK, 4-(methylnitrosamino)-1-(3-pyridyl)-1-butanone; Que, quercetin; Si α9, α9-nAChR knock down; siRNAs, small interfering RNAs; Sc, scrambled vector control.

Supporting Information Available: siRNAs and primers utilized for the experiments and their sequences. This material is available free of charge via the Internet at http://pubs.acs.org.

LITERATURE CITED

(1) Sagiv, S. K.; Gaudet, M. M.; Eng, S. M.; Abrahamson, P. E.; Shantakumar, S.; Teitelbaum, S. L.; Britton, J. A.; Bell, P.; Thomas, J. A.; Neugut, A. I.; Santella, R. M.; Gammon, M. D. Active and passive cigarette smoke and breast cancer survival. *Ann. Epidemiol.* **2007**, *17* (5), 385–393.

(2) Lin, Y.; Kikuchi, S.; Tamakoshi, K.; Wakai, K.; Kondo, T.; Niwa, Y.; Yatsuya, H.; Nishio, K.; Suzuki, S.; Tokudome, S.; Yamamoto, A.; Toyoshima, H.; Mori, M.; Tamakoshi, A. Active smoking, passive smoking, and breast cancer risk: findings from the Japan Collaborative Cohort Study for Evaluation of Cancer Risk. *J. Epidemiol.* **2008**, *18* (2), 77–83.

(3) Slattery, M. L.; Curtin, K.; Giuliano, A. R.; Sweeney, C.; Baumgartner, R.; Edwards, S.; Wolff, R. K.; Baumgartner, K. B.; Byers, T. Active and passive smoking, IL6, ESR1, and breast cancer risk. *Breast Cancer Res. Treat.* **2008**, *109* (1), 101–111.

(4) Armitage, A. K.; Dollery, C. T.; George, C. F.; Houseman, T. H.; Lewis, P. J.; Turner, D. M. Absorption and metabolism of nicotine from cigarettes. *Br. Med. J.* **1975**, *4* (5992), 313–316.

(5) Mei, J.; Hu, H.; McEntee, M.; Plummer, H.3rd; Song, P.; Wang, H. C. Transformation of non-cancerous human breast epithelial cell line MCF10A by the tobacco-specific carcinogen NNK. *Breast Cancer Res. Treat.* **2003**, *79* (1), 95–105.

(6) Siriwardhana, N.; Choudhary, S.; Wang, H. C. Precancerous model of human breast epithelial cells induced by NNK for prevention. *Breast Cancer Res. Treat.* **2008**, *109* (3), 427–441.

(7) Chen, R. J.; Ho, Y. S.; Guo, H. R.; Wang, Y. J. Rapid activation of Stat3 and ERK1/2 by nicotine modulates cell proliferation in human bladder cancer cells. *Toxicol. Sci.* **2008**, *104* (2), 283–293.

(8) Wong, H. P.; Yu, L.; Lam, E. K.; Tai, E. K.; Wu, W. K.; Cho, C. H. Nicotine promotes colon tumor growth and angiogenesis through beta-adrenergic activation. *Toxicol. Sci.* **2007**, *97* (2), 279–287.

(9) West, K. A.; Brognard, J.; Clark, A. S.; Linnoila, I. R.; Yang, X.; Swain, S. M.; Harris, C.; Belinsky, S.; Dennis, P. A. Rapid Akt activation by nicotine and a tobacco carcinogen modulates the

phenotype of normal human airway epithelial cells. *J. Clin. Invest.* **2003**, *111* (1), 81–90.
(10) Wong, H. P.; Yu, L.; Lam, E. K.; Tai, E. K.; Wu, W. K.; Cho, C. H. Nicotine promotes cell proliferation via α7-nicotinic acetylcholine receptor and catecholamine-synthesizing enzymes-mediated pathway in human colon adenocarcinoma HT-29 cells. *Toxicol. Appl. Pharmacol.* **2007**, *221* (3), 261–267.
(11) Schuller, H. M. Nitrosamines as nicotinic receptor ligands. *Life Sci.* **2007**, *80* (24−25), 2274–2280.
(12) Schuller, H. M.; Orloff, M. Tobacco-specific carcinogenic nitrosamines. Ligands for nicotinic acetylcholine receptors in human lung cancer cells. *Biochem. Pharmacol.* **1998**, *55* (9), 1377–1384.
(13) Hernandez-Ramirez, R. U.; Galvan-Portillo, M. V.; Ward, M. H.; Agudo, A.; Gonzalez, C. A.; Onate-Ocana, L. F.; Herrera-Goepfert, R.; Palma-Coca, O.; Lopez-Carrillo, L. Dietary intake of polyphenols, nitrate and nitrite and gastric cancer risk in Mexico City. *Int. J. Cancer* **2009**, *125* (6), 1424–1430.
(14) Shrubsole, M. J.; Lu, W.; Chen, Z.; Shu, X. O.; Zheng, Y.; Dai, Q.; Cai, Q.; Gu, K.; Ruan, Z. X.; Gao, Y. T.; Zheng, W. Drinking green tea modestly reduces breast cancer risk. *J. Nutr.* **2009**, *139* (2), 310–316.
(15) Pan, M. H.; Lin, C. C.; Lin, J. K.; Chen, W. J. Tea polyphenol (−)-epigallocatechin 3-gallate suppresses heregulin-β1-induced fatty acid synthase expression in human breast cancer cells by inhibiting phosphatidylinositol 3-kinase/Akt and mitogen-activated protein kinase cascade signaling. *J. Agric. Food Chem.* **2007**, *55* (13), 5030–5037.
(16) Kandaswami, C.; Lee, L. T.; Lee, P. P.; Hwang, J. J.; Ke, F. C.; Huang, Y. T.; Lee, M. T. The antitumor activities of flavonoids. *In Vivo* **2005**, *19* (5), 895–909.
(17) Kobayashi, T.; Nakata, T.; Kuzumaki, T. Effect of flavonoids on cell cycle progression in prostate cancer cells. *Cancer Lett.* **2002**, *176* (1), 17–23.
(18) Huang, Y. T.; Lee, L. T.; Lee, P. P.; Lin, Y. S.; Lee, M. T. Targeting of focal adhesion kinase by flavonoids and small-interfering RNAs reduces tumor cell migration ability. *Anticancer Res.* **2005**, *25* (3B), 2017–2025.
(19) Grozio, A.; Paleari, L.; Catassi, A.; Servent, D.; Cilli, M.; Piccardi, F.; Paganuzzi, M.; Cesario, A.; Granone, P.; Mourier, G.; Russo, P. Natural agents targeting the α7-nicotinic-receptor in NSCLC: a promising prospective in anti-cancer drug development. *Int. J. Cancer* **2008**, *122* (8), 1911–1915.
(20) Hiramoto, T.; Chida, Y.; Sonoda, J.; Yoshihara, K.; Sudo, N.; Kubo, C. The hepatic vagus nerve attenuates Fas-induced apoptosis in the mouse liver via α7 nicotinic acetylcholine receptor. *Gastroenterology* **2008**, *134* (7), 2122–2131.
(21) Aerts, J. L.; Gonzales, M. I.; Topalian, S. L. Selection of appropriate control genes to assess expression of tumor antigens using real-time RT-PCR. *Biotechniques* **2004**, *36*, (1), 84−86, 88, 90−91.
(22) Ho, Y. S.; Chen, C. H.; Wang, Y. J.; Pestell, R. G.; Albanese, C.; Chen, R. J.; Chang, M. C.; Jeng, J. H.; Lin, S. Y.; Liang, Y. C.; Tseng, H.; Lee, W. S.; Lin, J. K.; Chu, J. S.; Chen, L. C.; Lee, C. H.; Tso, W. L.; Lai, Y. C.; Wu, C. H. Tobacco-specific carcinogen 4-(methylnitrosamino)-1-(3-pyridyl)-1-butanone (NNK) induces cell proliferation in normal human bronchial epithelial cells through NFκB activation and cyclin D1 up-regulation. *Toxicol. Appl. Pharmacol.* **2005**, *205* (2), 133–148.
(23) John, M.; Geick, A.; Hadwiger, P.; Vornlocher, H. P.; Heidenreich, O. Gene silencing by RNAi in mammalian cells. *Curr. Protoc. Mol. Biol.* **2003**, Chapter 26, Unit 26 2.
(24) Narayan, S.; Jaiswal, A. S.; Kang, D.; Srivastava, P.; Das, G. M.; Gairola, C. G. Cigarette smoke condensate-induced transformation of normal human breast epithelial cells in vitro. *Oncogene* **2004**, *23* (35), 5880–5889.
(25) Liu, Z.; Yu, X.; Shaikh, Z. A. Rapid activation of ERK1/2 and AKT in human breast cancer cells by cadmium. *Toxicol. Appl. Pharmacol.* **2008**, *228* (3), 286–294.
(26) Sun, X.; Ritzenthaler, J. D.; Zhong, X.; Zheng, Y.; Roman, J.; Han, S. Nicotine stimulates PPARβ/δ expression in human lung carcinoma cells through activation of PI3K/mTOR and suppression of AP-2α. *Cancer Res.* **2009**, *69* (16), 6445–6453.
(27) Arredondo, J.; Nguyen, V. T.; Chernyavsky, A. I.; Jolkovsky, D. L.; Pinkerton, K. E.; Grando, S. A. A receptor-mediated mechanism of nicotine toxicity in oral keratinocytes. *Lab. Invest.* **2001**, *81* (12), 1653–1668.
(28) Arredondo, J.; Nguyen, V. T.; Chernyavsky, A. I.; Bercovich, D.; Orr-Urtreger, A.; Kummer, W.; Lips, K.; Vetter, D. E.; Grando, S. A. Central role of α7 nicotinic receptor in differentiation of the stratified squamous epithelium. *J. Cell Biol.* **2002**, *159* (2), 325–336.
(29) Arredondo, J.; Hall, L. L.; Ndoye, A.; Nguyen, V. T.; Chernyavsky, A. I.; Bercovich, D.; Orr-Urtreger, A.; Beaudet, A. L.; Grando, S. A. Central role of fibroblast α3 nicotinic acetylcholine receptor in mediating cutaneous effects of nicotine. *Lab. Invest.* **2003**, *83* (2), 207–225.
(30) Wei, P. L.; Chang, Y. J.; Ho, Y. S.; Lee, C. H.; Yang, Y. Y.; An, J.; Lin, S. Y. Tobacco-specific carcinogen enhances colon cancer cell migration through α7-nicotinic acetylcholine receptor. *Ann. Surg.* **2009**, *249* (6), 978–985.
(31) Wang, L.; Lee, I. M.; Zhang, S. M.; Blumberg, J. B.; Buring, J. E.; Sesso, H. D. Dietary intake of selected flavonols, flavones, and flavonoid-rich foods and risk of cancer in middle-aged and older women. *Am. J. Clin. Nutr.* **2009**, *89* (3), 905–912.
(32) Androutsopoulos, V. P.; Mahale, S.; Arroo, R. R.; Potter, G. Anticancer effects of the flavonoid diosmetin on cell cycle progression and proliferation of MDA-MB 468 breast cancer cells due to CYP1 activation. *Oncol. Rep.* **2009**, *21* (6), 1525–1528.
(33) Androutsopoulos, V.; Wilsher, N.; Arroo, R. R.; Potter, G. A. Bioactivation of the phytoestrogen diosmetin by CYP1 cytochromes P450. *Cancer Lett.* **2009**, *274* (1), 54–60.
(34) Du, G. J.; Song, Z. H.; Lin, H. H.; Han, X. F.; Zhang, S.; Yang, Y. M. Luteolin as a glycolysis inhibitor offers superior efficacy and lesser toxicity of doxorubicin in breast cancer cells. *Biochem. Biophys. Res. Commun.* **2008**, *372* (3), 497–502.
(35) Lin, C. W.; Hou, W. C.; Shen, S. C.; Juan, S. H.; Ko, C. H.; Wang, L. M.; Chen, Y. C. Quercetin inhibition of tumor invasion via suppressing PKC δ/ERK/AP-1-dependent matrix metalloproteinase-9 activation in breast carcinoma cells. *Carcinogenesis* **2008**, *29* (9), 1807–1815.
(36) Samy, R. P.; Gopalakrishnakone, P.; Ignacimuthu, S. Anti-tumor promoting potential of luteolin against 7,12-dimethylbenz-(*a*)anthracene-induced mammary tumors in rats. *Chem.−Biol. Interact.* **2006**, *164* (1−2), 1–14.

Received for review September 8, 2009. Revised manuscript received October 21, 2009. Accepted October 26, 2009. This work was supported by the National Science Council, NSC 96-2628-B-038-003-MY3(1-3) and NSC 98-2320-B-038-006-MY3(1-3) to Y.-S.H. and NSC 97-2320-B-038-012-MY2(1-2) to Y.-Y.Y. and the Shin Kong Wu Ho-Su Memorial Hospital SKH-TMU-97-12.